

UC Irvine

UC Irvine Electronic Theses and Dissertations

Title

A Deep Learning Approach to Estimate Blood Pressure from PPG Signals

Permalink

<https://escholarship.org/uc/item/0pd0x3rr>

Author

Tazarv, Ali

Publication Date

2022

Copyright Information

This work is made available under the terms of a Creative Commons Attribution License, available at <https://creativecommons.org/licenses/by/4.0/>

Peer reviewed|Thesis/dissertation

UNIVERSITY OF CALIFORNIA,
IRVINE

A Deep Learning Approach to Estimate Blood Pressure from PPG Signals

THESIS

submitted in partial satisfaction of the requirements
for the degree of

MASTER OF SCIENCE

in Electrical Engineering

by

Ali Tazarv

Thesis Committee:
Professor Sameer Singh, Chair
Professor Matthew Harding
Professor Ender Ayanoglu

2022

DEDICATION

To my parents for their unconditional love, incredible sacrifices, and support.

TABLE OF CONTENTS

	Page
LIST OF FIGURES	iv
LIST OF TABLES	v
ACKNOWLEDGMENTS	vi
ABSTRACT OF THE THESIS	vii
1 Introduction	1
1.1 PPG signals and Blood Pressure	2
1.2 Related Work	4
1.3 Overview and Contributions of this Thesis	5
2 Proposed Model	7
2.1 Pre-processing	7
2.2 Deep Learning	9
3 Data, Metrics, and Experimental Results	11
3.1 Datasets	11
3.1.1 MIMIC v.3 2015	11
3.1.2 The University of Queensland Vital Signs Dataset:	12
3.2 Experimental Results	13
4 Conclusions and Future Work	18
Bibliography	20

LIST OF FIGURES

	Page
1.1 Schematics of PPG sensor design	2
1.2 ABP and PPG Correlation	3
2.1 Overview of the proposed method to estimate BP from single channel PPG signal	8
2.2 Splitting PPG signals into 8s windows, t_i is the sample at timestamp i	8
3.1 Example of PPG (a portion of a normalized signal) and the corresponding raw ABP signal from MIMIC-II dataset	12
3.2 Distribution of Systolic BP and Diastolic BP	13
3.3 Prediction Error for SBP (left), and DBP (right)	16
3.4 Bland-Altman plot for SBP and DBP	16

LIST OF TABLES

	Page
3.1 Performance comparison with prior works	14
3.2 BHS Standard [27] vs. our results	17
3.3 Comparison of results with AAMI Standard [7]	17

ACKNOWLEDGMENTS

Foremost, I would like to express my sincere gratitude to Professors Marco Levorato, Matthew Harding, and Sameer Singh, whom I had the opportunity to learn research work under their supervision in the past few years.

I would like to thank my parents: Mohammad and Soori, and my brothers and sister for their love and support throughout the years of my education. I would like to thank my friends whom without, life could be much more difficult in a new country and far from the family.

I thank the Institute of Electrical and Electronics Engineers (IEEE) for giving me permission to include my previously published papers in this thesis.

ABSTRACT OF THE THESIS

A Deep Learning Approach to Estimate Blood Pressure from PPG Signals

By

Ali Tazarv

Master of Science in Electrical Engineering

University of California, Irvine, 2022

Professor Sameer Singh, Chair

Blood Pressure (BP) is one of the four primary vital signs indicating the status of the body vital (life-sustaining) functions. BP is difficult to continuously monitor using a sphygmomanometer (i.e. a blood pressure cuff), especially in everyday-setting. However, other health signals which can be easily and continuously acquired, such as photoplethysmography (PPG), show some similarities with the Aortic Pressure waveform. Based on these similarities, in recent years several methods were proposed to predict BP from the PPG signal. Building on these results, we propose an advanced personalized data-driven approach that uses a three-layer deep neural network to estimate BP based on PPG signals. Different from previous work, the proposed model analyzes the PPG signal in time-domain and automatically extracts the most critical features for this specific application, then using a variation of recurrent neural networks called Long-Short-Term-Memory (LSTM) to map the extracted features to the BP value associated with that time window. Experimental results on two separate standard hospital datasets, yielded absolute errors mean and absolute error standard deviation for systolic and diastolic BP values outperforming all prior approaches.

Chapter 1

Introduction

Hypertension, defined as systolic blood pressure (SBP) larger than 140mmHg, or diastolic blood pressure (DBP) larger than 90mmHg (SBP and DBP are the two values used for measuring BP), or taking antihypertensive medication [2], is estimated to have caused 9.4 million annual deaths globally, 17% of the total death in 2012 and 7% of total disability adjusted life years (DALYs) [28]. If left uncontrolled, hypertension causes stroke, myocardial infarction (MI), cardiac failure, dementia, renal failure and even blindness. In adults, hypertension after diabetes is the second reason to increase the risk of cardiovascular disease (CVD) and several types of cancer, as well as multiple non-fatal diseases. Hypertension has been increasing in recent years. By 2030, 40.5% of the US population is projected to have some form of CVD [10]. The prevalence of hypertension is highest in some low-income populations [28]. While people with the risk of hypertension need to measure their blood pressure frequently, conventional cuff-based BP measurement devices are expensive and inconvenient for continuous monitoring. Thus the development of alternative methods is necessary.

Blood Pressure (BP) – commonly reported in mmHg – is a quasi-periodic signal in sync with the heart activities. The upper peak in each period is called the Systolic Blood Pressure



Figure 1.1: Schematics of PPG sensor design

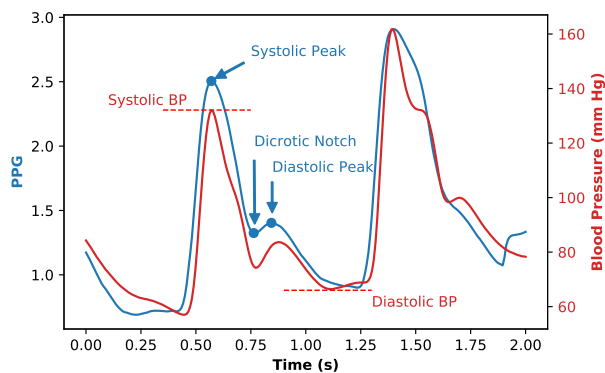
(SBP), and the lower bound in each period is called Diastolic Blood Pressure (DBP).

1.1 PPG signals and Blood Pressure

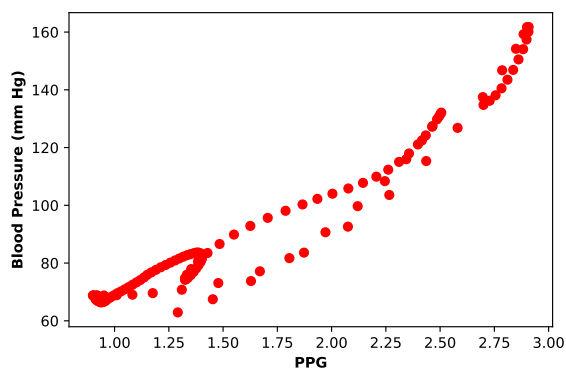
While the BP signal is difficult to acquire continuously in everyday settings, Photoplethysmography (PPG) is a non-invasive optical method that measures a related signal: temporal variations of blood volume in the vessels and tissues. PPG signals are obtained from pulse oximeters, emitting visible light (LED) on the skin and measuring the micro-variations in the transmitted or reflected light intensity through a Photo-Diode, as depicted in Figure 1.1. PPG sensors are small in size and low cost to build, and they exist in most of the newer smart wearables (e.g. smartwatches, activity trackers, and smart rings).

In recent years, there has been an extensive body of research studying similarities and correlation of PPG signals and Aortic Pressure waveforms, and furthermore, prediction of SBP and DBP based on PPG signals. An example of experimental waveforms for a subject is presented in Figure 1.2. As can be seen from this example, since both signals are originating from the same source (heart beats), they can be highly correlated with each other. However, since Aortic and PPG are generally measured from different parts of the body (e.g. arm vs. wrist), and using different devices, they are typically out of phase. Figure 1.2 is based on experimental data after time-shift alignment. A few recent methods, such as the one in [33], have been proposed to automatically compensate for the phase difference.

Considering the architecture of PPG sensors in Figure 1.1, they are vulnerable to motion



(a) Signals in the time Domain



(b) (PPG, ABP) samples

Figure 1.2: ABP and PPG Correlation

artifacts (MA) which result in distortion in the signal fidelity. MA originate from a number of factors [6]; the physical activity which might change the location of the sensor on the skin, light leaking through the gap between the sensor and the skin, and the change in the blood flow because of the physical movements are the most important factors of MA. The overall effect is that MA might dominate the original PPG signal, which was intended to be an indicator of the heart activities. Properties of PPG signal and some of its applications are reviewed in [1].

1.2 Related Work

Several methods to estimate BP from PPG have been proposed and studied in prior works. For example in [15], [18] and [23], the authors propose BP estimation methods based on Pulse Transit Time (PTT). PTT is defined as the time required for the blood pressure wave to travel from the source (heart) to the wrist (where the PPG signal is recorded, and it is measured by the time lag between the Electrocardiography (ECG) and PPG signals. In [25], authors consider every sample point in one cycle as a separate feature and use Principal Component Analysis (PCA) to reduce the number of features, and then apply regression algorithms on the set of reduced features. In another work [29], authors propose a list of some potential features of the PPG signals (e.g. area under the curve, the time length of certain points on the signal in one cycle, etc.), and then use an autoencoder to reduce the number of expressive features. In the end stage, they use a feed-forward neural network to predict BP based on a reduced set of features.

The available solutions for estimating BP based on PPG signals in the literature are to first extract a set of expressive features from PPG signals, and then estimate SBP and DBP based on those features. A shortcoming of these approaches is that they may fail to capture all the expressive features in the raw PPG signal from an application point of view. In other words, there might be some informative features in the raw PPG signal which can play important role in BP estimation, but are not included in the initial feature set (because it is a limited list). Even in [25] the authors start with all the sample points in each cycle and then apply PCA on those, the feature reduction procedure is not optimized for the BP estimation application, as it is a general data compression method. Additionally, none of these approaches exploit possible characterizations of the PPG as a time-series signal.

Different from these contributions, the proposed machine learning based method automatically extracts features from the signal and analyzes temporal dependencies using an advanced

neural architecture. Machine learning methods are broadly used in numerous healthcare applications from preprocessing and cleaning of the data, to monitoring and detection of various physiological factors and event [32][14].

In addition to BP estimation, some of the other popular applications of PPG signals are Heart Rate extraction [35][3], Bio-metric Identification [3], arterial oxygen saturation [1], determining arterial stiffness [12], mental health monitoring and tracking [31], and other bio-medical applications [24].

1.3 Overview and Contributions of this Thesis

In this thesis, we propose a new framework to address the shortcomings mentioned above. Specifically, the proposed approach makes the following advancements with respect to prior literature: (i) The proposed method utilizes a Convolutional Neural Network (CNN) layer, which “learns” the most critical features of the PPG signal for this specific application (BP estimation) in a nonlinear and efficient way, as part of an optimization problem; (ii) We adopt a Long-Short Term Memory (LSTM) neural network model to capture temporal inter-dependencies and condensate past information in a seamless and fully automated way.

We train and test the model for each subject separate from others. We apply the proposed framework on two standard hospital datasets. The proposed model on MIMIC-II dataset including 20 subjects, gives prediction error ($MAE \pm SDAE$) of 3.70 ± 3.07 mmHg and 2.02 ± 1.76 mmHg, for SBP and DBP values respectively. Also on UQVSD dataset, prediction errors ($MAE \pm SDAE$) are 3.70 ± 3.07 mmHg and 2.02 ± 1.76 mmHg, for SBP and DBP respectively. To the best of our knowledge, these results outperform other methods available in the literature.

The rest of the thesis is organized as follows. Chapter 2 explains our proposed framework

and the methodology to solve the estimation problem. Chapter 3 explains the datasets we used to evaluate the proposed model and the results of the evaluation and comparison with state-of-the-art methods. And Chapter 4 concludes the thesis.

Chapter 2

Proposed Model

We propose a Deep Learning architecture to estimate blood pressure values directly from PPG signals. Figure 2.1 presents the block diagram of the proposed model. The method is composed of the following blocks and components: (1) Signal Pre-processing Block; (2) Machine Learning Block composed of a Smart Feature extraction (CNN) and a Time Series Analysis (LSTM) module; and (3) Model Evaluation block. We explain the first two blocks here and talk about Evaluation block later in Chapter 3.

2.1 Pre-processing

The input PPG and ABP signals are assumed to be temporal waveforms with a sampling frequency $f_s = 20Hz$. Since both signals originate from a bio-mechanical source (heart activities), we do not expect to see high frequency elements in their waveforms. Thus, higher frequency elements are likely due to noise. Additionally, since the PPG is a relative signal and its DC offset (mean value) does not have an interpretation of our interest, we eliminate the mean value of the signal (the zero frequency element). There are many popular methods

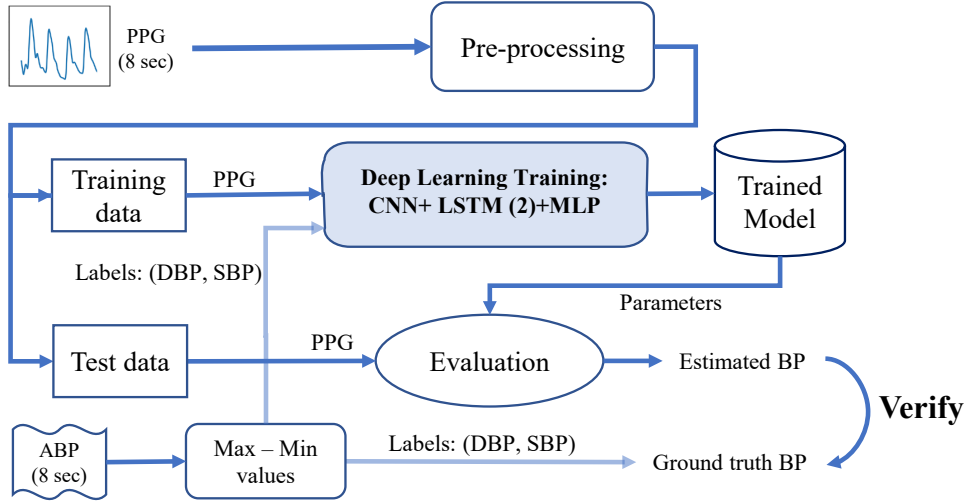


Figure 2.1: Overview of the proposed method to estimate BP from single channel PPG signal

to eliminate a predefined frequency range from a signal. Herein, we use a traditional Fourier Transform (FFT)-based approach. In the PPG signal, we set a band-pass filter eliminating the frequencies outside the range 0.1 – 8 Hz. The resulting waveform still contains all the information necessary for our estimation, while being affected by a smaller noise energy. In preprocessing the Aortic Pressure signal, we apply a low-pass filter with cut-off frequency 5Hz to the raw signal to eliminate sharp peaks in the signal. After these steps, we split both the PPG and ABP into chunks (windows or frames) of 8 s with a step of 2s, resulting in 6s overlaps between consecutive windows (gray shaded part in Figure 2.2).

Each window is composed of 160 sample points ($8s \times 20Hz$) which we use as the model input, either as training or test data. In the ABP signal, the signal is passed through a 1 Hz digital lowpass filter (to eliminate large instant changes in the BP), and then the maximum

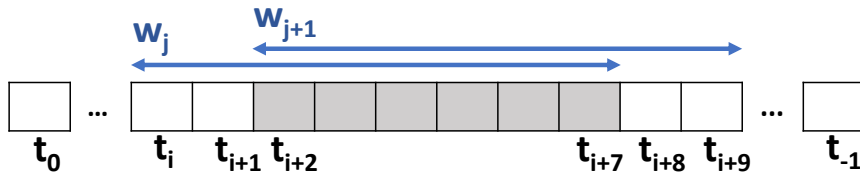


Figure 2.2: Splitting PPG signals into 8s windows, t_i is the sample at timestamp i .

and minimum value in each window (Fig. 1.2a), are labeled as the Systolic and Diastolic BP respectively for that sample.

2.2 Deep Learning

Deep Neural Networks, and primarily including Multi-Layer-Perceptron (MLP), Convolutional Neural Network (CNN) and Recurrent Neural Network (RNN) architectures, facilitate task-adapted feature representation of the data. CNN, which was specifically designed to deal with variability of 2D shapes, in [19] is shown to perform well on 1D data and outperform other existing approaches for certain tasks. CNN consists of an initial layer of convolutional filters – boxes of certain sizes sF , with certain sets of trainable weights which slide over the input data – followed by an activation function (e.g. Rectified Linear Units), a pooling layer (down sampling) with pool size sP , and eventually a fully connected (Dense) layer. Stacking multiple convolutional layers results in a non-linear, smart and task-adaptive method to extract features from data [22].

RNNs are an effective choice for time series data analysis, since they learn contextual patterns in the input from previous time steps. Unlike feed-forward networks, RNNs use their internal states to process temporal sequences of the input. However, learning to store information over extended time intervals via recurrent back-propagation may necessitate an excessive training time, due to the insufficient decaying error gradient back-flow (vanishing gradient) discussed in [11].

Long-Short-Term-Memory (LSTM) is a variation of RNN and solves this issue by using memory blocks, for which the trainable “forget gate”, “input gate” and “output gate” control which parts of the data are worth saving and which parts are not, this idea solves the issue of vanishing gradient mentioned above, and the result is a strong tool to learn and track

long-term inter-dependencies in the input data (e.g. time series data). The combination of CNN with a subsequent LSTM has been shown to perform well on PPG signals. As an example, in [3] authors use a similar architecture for estimating heart-rate and Bio-metric ID based on PPG signals. Herein, we use a similar structure applied to the problem at hand.

The model is trained in Python environment (version 3.6.3) and implemented using Keras 2.2.4 [4], with Tensorflow 1.3.1 backend. The CNN layer starts with a 1-D filtering operation with filter size $sF = 15$ followed by a Rectified Linear Unit (RELU) [26] as activation function, a batch-normalization layer [13], a max-pooling layer with pool size $sP = 4$, and finally a dropout layer [30] with $dropout_rate = 0.1$. The Max-pooling layer is a type of down sampling: as we set sP to be equal to 4, the layer looks at the 4 elements of each filter (non-overlapping), keeps the maximum element and discards the rest, so that the output length is one fourth of the input length. Unlike some other common deep network layers (e.g. Dense), the Max-pooling layer does not have trainable weights. Dropout layers are probabilistic masks that in every gradient update (mini-batch) block a portion of the nodes (set their output equal to zero). In our implementation, the $dropout_rate = 0.1$ means that in every gradient update, there is a 10% chance for each node in the layer to be dropped (blocked, or set to zero). These two layers (Max-pooling and Dropout) are well-known methods used to avoid overfitting.

Our LSTM network is composed of two series of identical LSTM layers. Each of them has 64 units (nU), with *tanh* as the activation function for the hidden state data and output data, and *hard-sigmoid* as the recurrent activation functions for the forget, input, output gates.

The model was trained using Adam optimizer [16]. Batch size was set to 20 to balance the training time vs noisiness of gradient updates trade-off. The hyperparameters mentioned above and also the number of layers for each network (CNN and LSTM), were optimized by means of a grid search. Changing the hyperparameters (e.g. sF , nU, sP , etc.) or the number of layers did not result in an improved final output.

Chapter 3

Data, Metrics, and Experimental Results

3.1 Datasets

To evaluate the accuracy and efficiency of the proposed method, we used two publicly accessible real life datasets. Each of these datasets are collected from a number of participants in hospital settings. We briefly explain each of them in this section.

3.1.1 MIMIC v.3 2015

Multi-parameter Intelligent Monitoring in Intensive Care, provided by [9]. The MIMIC-II dataset includes health-care information and signals of thousands of patients at a number of hospitals between the years 2001 and 2008. Part of this large dataset, including PPG, Arterial Blood Pressure (ABP) and Electrocardiogram (ECG) signals is extracted and used in another work [15]. An example of PPG and corresponding ABP signals from this dataset

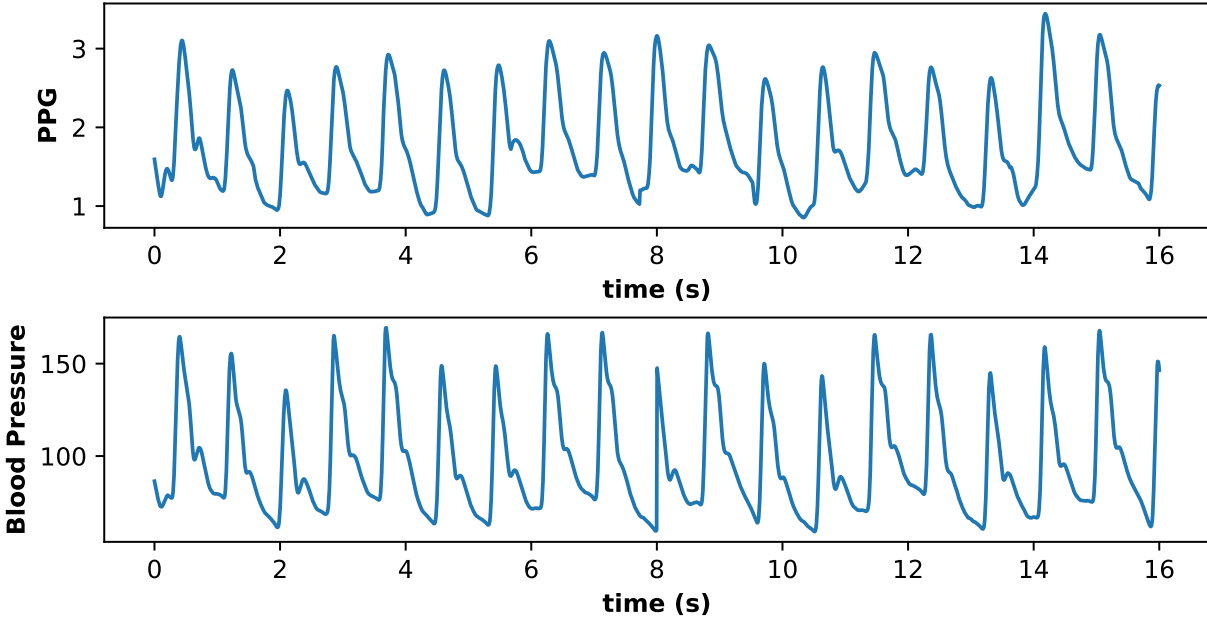


Figure 3.1: Example of PPG (a portion of a normalized signal) and the corresponding raw ABP signal from MIMIC-II dataset

is given in Figure 3.1 (PPG in that figure is a portion of a normalized raw signal). These signals are originally recorded at a sampling frequency $f_s=125$ Hz, with a minimum accuracy of 8 bits. We randomly selected data corresponding to 20 different subjects -five minutes long each- from this dataset to test our model.

3.1.2 The University of Queensland Vital Signs Dataset:

This dataset covers a wide range of BP values, recorded from 32 surgical patients in duration ranging from 13 minutes to 5 hours, at the Royal Adelaide Hospital, Australia [20]. This dataset is recorded at the sampling frequency $f_s = 100Hz$. We used 49 measurements (10 minute intervals) from this dataset.

The majority of studies on this topic have used one of these two datasets. However, details of how portions of these datasets were selected for experiments were not revealed. We acknowledge that the data we used for our experiment, might not be exactly matching the

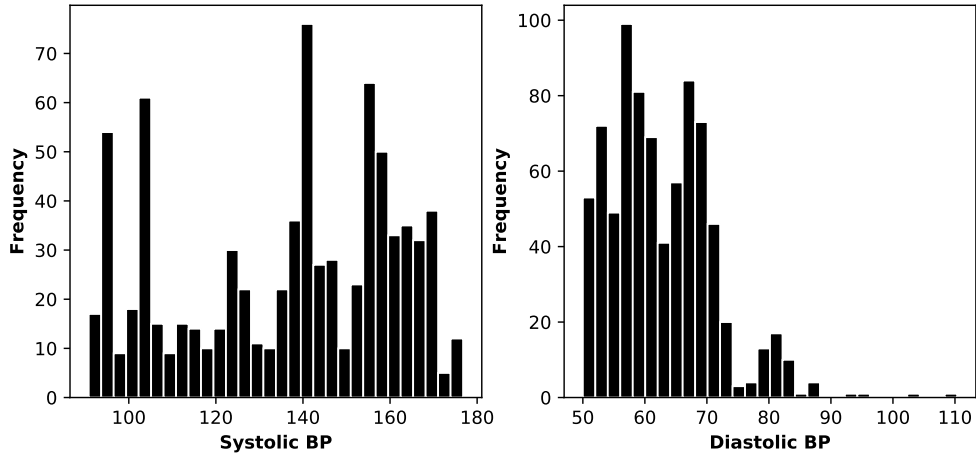


Figure 3.2: Distribution of Systolic BP and Diastolic BP

data used in similar studies. But in order to conduct a fair comparison, we picked a portion of each dataset randomly.

For both datasets, we re-sampled the PPG and ABP signals at 20 Hz, and re-adjusted the timings [33] (in most of the records PPG and ABP were off by around 0.25-0.35 s). The distribution of BP in MIMIC-II data (that we used in this experiment) is given in Figure 3.2. After these steps, the resulting PPG signals and ABP values are ready to be used for training and evaluation of our method.

3.2 Experimental Results

The preprocessed PPG signals and BP values from both datasets (section 3.1) are further normalized to zero mean and unit variance before being used as the input to the network. The relevant linear and nonlinear features of the input data are extracted through a CNN network, and then these features are given to a two layer LSTM network to do the time series analysis. What is important to consider here is that unlike conventional methods, feature extraction is performed as part of the training process; the trainable weights in the CNN are optimized to extract the most important features of the PPG signal, and by important we

Table 3.1: Performance comparison with prior works

Work	Dataset	SBP		DBP	
		MAE	SD	MAE	SD
[8]	MIMIC-II	4.47	6.85	3.21	4.72
[21]	MIMIC-II	8.54	-	4.34	-
[25]	MIMIC-II	3.97	7.99	2.43	3.37
[17]	MIMIC-II	3.80	3.46	2.21	2.09
Our work	MIMIC-II	3.70	3.07	2.02	1.76
[34]	UQVSD	11.64	8.20	7.62	6.78
[5]	UQVSD	4.77	7.68	3.67	5.69
Our work	UQVSD	3.91	4.78	1.99	2.45

mean they are informative toward the estimation of the BP values. We perform *leave-one-window-out* validations. Hence, one 8s time window is kept separate, and training is done on the rest of data. Then, the trained model is evaluated on the test sample. Also for training, we do not use three time windows on each side of test sample, to account for the 6s overlap between two consecutive time windows. With this strategy, the training data and test data will be completely separate from one another. We are training and testing the model for each subject independently from the others. The performance of the network is evaluated using the following three metrics:

Absolute Error (AE): for each test sample, AE is defined as $AE_i = |BP_{T_i} - BP_{E_i}|$, in which BP_{T_i} is the true or target blood pressure, and BP_{E_i} is the estimated blood pressure when window number i is held out as the test sample. Consequently the mean value of AE_i and the standard deviation over all `number_of_samples` iterations (for each subject), and then over all subjects are calculated and reported in the Table 3.1. Mean of AE would be rough estimate of the error value on predictions, and standard deviation of AE would tell how robust and reliable the method is. A model is selected as a strong predictor, if it produces small MAE and $SDAE$ values. The method proposed in this thesis, to the best of our knowledge, outperforms all other currently available frameworks and techniques.

BHS: As a second metric, we consider a standard commonly used for blood pressure measurements accuracy, provided by the British Hypertension Society (BHS) [27], which grades the measurement accuracy into three groups (A-C). This metric measures the fraction of measurements (or estimations) which are within a certain range – 5, 10 and 15 mmHg – of the target values for unobserved data. Based on this metric, our proposed model (to the best of our knowledge) is the only method that gets Grade **A** for both SBP and DBP (in predictions based on PPG only). Detailed results are given in Table 3.2. For comparison authors in [25] report grade *A* for DBP and below *C* for SBP estimation on MIMIC-II dataset. Also authors in [5] report grade *A* for DBP, and *B* for SBP estimation on UQVSD dataset.

AAMI: As the third metric, we consider a different standard provided by the US Association for the Advancement of Medical Instrumentation (AAMI) [7]. Based on this Standard, a measurement algorithm is valid if the ME (Mean Error) of the measurements is below 5 mmHg and the SD of Errors is smaller than 8 mmHg. The results are presented in Table 3.3. Our model passes the AAMI standard criteria for both SBP and DBP on both dataset. For comparison, our proposed model produces better error values (lower mean and σ) compared to [5] on UQVSD data. On MIMIC-II dataset we get lower error σ but higher error mean compared to [25].

The distribution of the prediction error for one subject from the MIMIC-II dataset is depicted in Figure 3.3. Based on the histograms, prediction errors are mostly small. However, in some rare cases (less than 1% of times) the estimation error for SBP goes beyond the 20 mmHg range from the target value. For DBP, that never happened in our experiments.

The Bland-Altman plot for the predictions on the same subject is shown in Figure 3.4. Predictions on lower values of BP – left side of each plot - are more reliable (smaller error). Note that these data points correspond to the times that the subject is likely to be less active (potentially at rest), at which the PPG signal is expected to be less noisy and more reliable.

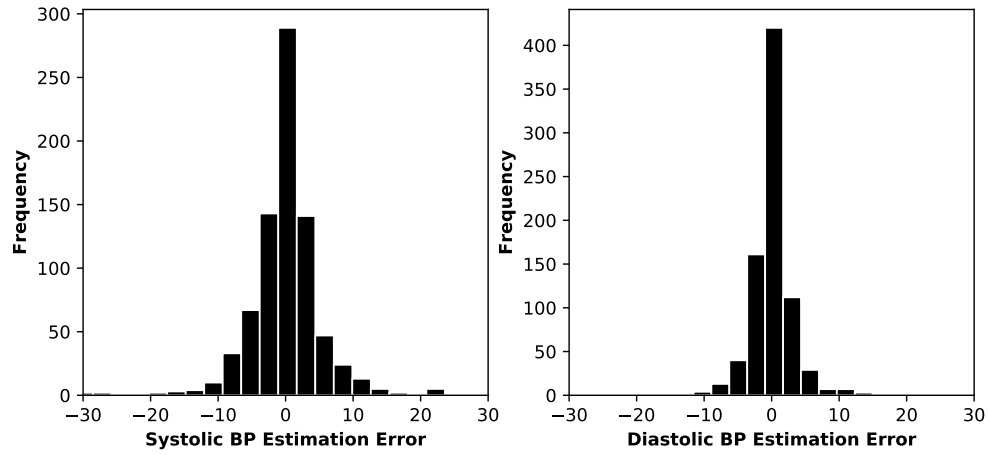


Figure 3.3: Prediction Error for SBP (left), and DBP (right)

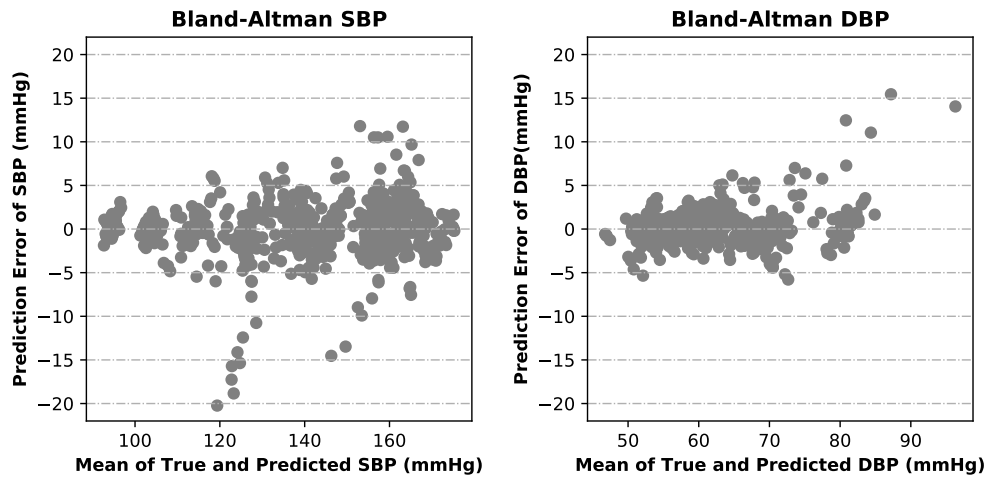


Figure 3.4: Bland-Altman plot for SBP and DBP

Table 3.2: BHS Standard [27] vs. our results

(a) BHS Standard Minimum Requirements

Cumulative Percentage Error			
	≤ 5 mmHg	≤ 10 mmHg	≤ 15 mmHg
Grade A	60%	85%	95%
Grade B	50%	75%	90%
Grade C	40%	65%	85%

(b) Our results on the two datasets

Cumulative Percentage Error (Grade)				
Dataset	Signal	≤ 5 mmHg	≤ 10 mmHg	≤ 15 mmHg
MIMIC-II	SBP	77% (A)	92% (A)	96% (A)
	DBP	93% (A)	97% (A)	99% (A)
UQVSD	SBP	75% (A)	92% (A)	96% (A)
	DBP	92% (A)	98% (A)	99% (A)

Table 3.3: Comparison of results with AAMI Standard [7]

		Mean Error	σ of Error
AAMI Criteria:		≤ 5	≤ 8
MIMIC-II	SBP	0.21	6.27
	DBP	0.24	3.40
UQVSD	SBP	0.52	6.16
	DBP	0.20	3.15

Chapter 4

Conclusions and Future Work

Hypertension or high blood pressure is closely related with cardiovascular disease. While continuous and portable BP monitoring is of high importance, conventional cuff-based BP measurement devices are primarily confined to clinical settings. The method proposed in this thesis is a cuff-less, noninvasive and feasible method which estimates Blood Pressure with high accuracy based on only PPG signals. PPG sensors are simple and low cost, and are integrated in most of newer smart watches and wearable devices. We use Convolutional Neural Network to automatically extract the best features of the input, and then use a LSTM network to analyze a time series analysis of the extracted features. Results of the proposed method outperform previous methods that only use PPG signal as input. Importantly, the proposed method ranks as **A** in the BHS Standard for both SBP and DBP, complies with the AAMI Standard, and also outperforms all the other similar works in terms of prediction error (as well as BHS criteria).

Wearable devices designed in recent years are able to capture a variety of health signals including PPG, electrocardiogram (ECG), electromyography (EMG), and more. Deep learning architectures applied on these signals along with personalization methods can be utilized to

monitor various health factors such as mental health, blood glucose levels, oxygen saturation levels, and to detect abnormalities. In addition, health signals contain subjective patterns, which along with feasibility of wearable sensors, makes them good candidates to be used for identification purposes.

Personalization is a solid direction to improve the accuracy and performance of these models. However, building reliable subjective datasets that include the target variables is always a challenge. Another challenge of working with health signals from wearables is the high levels of noise which mainly originates from physical motions. Both of these are active areas in research.

Lastly, even though the processing power required to execute the model (and more importantly, to keep it updated with the new subjective data) might be expensive to be executed on the edge layer in an IoT architecture, in certain scenarios the data can be transferred to the cloud, and the prediction output can be sent back to the user through a smart-watch or smart-phone, all in real-time. The development of such architecture is left to future work.

Bibliography

- [1] J. Allen. Photoplethysmography and its application in clinical physiological measurement. *Physiological measurement*, 28(3):R1, 2007.
- [2] E. J. Benjamin et al. Heart disease and stroke statistics—2018 update: A report from the american heart association. *Circulation*, 137(12):e67–e492, 2018.
- [3] D. Biswas et al. Cornet: Deep learning framework for ppg-based heart rate estimation and biometric identification in ambulant environment. *IEEE Transactions on Biomedical Circuits and Systems*, 13(2):282–291, April 2019.
- [4] F. Chollet et al. Keras. <https://keras.io>, 2015.
- [5] K. Duan et al. A feature exploration methodology for learning based cuffless blood pressure measurement using photoplethysmography. In *2016 38th Annual International Conference of the IEEE Engineering in Medicine and Biology Society (EMBC)*, pages 6385–6388, Aug 2016.
- [6] M. Elgendi. On the analysis of fingertip photoplethysmogram signals. *Current cardiology reviews*, 8(1):14–25, 2012.
- [7] A. for the Advancement of Medical Instrumentation et al. American national standard. manual, electronic or automated sphygmomanometers. *ANSI/AAMI SP10-2002/A1*, 2003.
- [8] A. Gaurav, M. Maheedhar, V. N. Tiwari, and R. Narayanan. Cuff-less ppg based continuous blood pressure monitoring — a smartphone based approach. In *2016 38th Annual International Conference of the IEEE Engineering in Medicine and Biology Society (EMBC)*, pages 607–610, Aug 2016.
- [9] A. L. Goldberger et al. Physiobank, physiotoolkit, and physionet. *Circulation*, 101(23):e215–e220, 2000.
- [10] P. A. Heidenreich et al. Forecasting the future of cardiovascular disease in the united states. *Circulation*, 123(8):933–944, 2011.
- [11] S. Hochreiter and J. Schmidhuber. Long short-term memory. *Neural Computation*, 9(8):1735–1780, 1997.

- [12] M. Huotari et al. Photoplethysmography and its detailed pulse waveform analysis for arterial stiffness. *Journal of Structural Mechanics*, 44(4):345–362, 2011.
- [13] S. Ioffe and C. Szegedy. Batch normalization: Accelerating deep network training by reducing internal covariate shift. *CoRR*, abs/1502.03167, 2015.
- [14] K. Joshi, A. Javani, J. Park, V. Velasco, B. Xu, O. Razorenova, and R. Esfandyarpour. A machine learning-assisted nanoparticle-printed biochip for real-time single cancer cell analysis. *Advanced Biosystems*, 4(11):2000160, 2020.
- [15] M. Kachuee, M. M. Kiani, H. Mohammadzade, and M. Shabany. Cuff-less high-accuracy calibration-free blood pressure estimation using pulse transit time. In *2015 IEEE International Symposium on Circuits and Systems (ISCAS)*, pages 1006–1009, May 2015.
- [16] D. P. Kingma and J. Ba. Adam: A method for stochastic optimization. *CoRR*, abs/1412.6980, 2014.
- [17] Y. Kurylyak, F. Lamonaca, and D. Grimaldi. A neural network-based method for continuous blood pressure estimation from a ppg signal. In *2013 IEEE International Instrumentation and Measurement Technology Conference (I2MTC)*, pages 280–283, May 2013.
- [18] J. Lass et al. Continuous blood pressure monitoring during exercise using pulse wave transit time measurement. In *The 26th Annual International Conference of the IEEE Engineering in Medicine and Biology Society*, volume 1, pages 2239–2242. IEEE, 2004.
- [19] Y. Lecun et al. Gradient-based learning applied to document recognition. *Proceedings of the IEEE*, 86(11):2278–2324, Nov 1998.
- [20] D. Liu, M. Görge, and S. A. Jenkins. University of queensland vital signs dataset: Development of an accessible repository of anesthesia patient monitoring data for research. *Anesthesia & Analgesia*, 114(3):584–589, 2012.
- [21] M. Liu, L. Po, and H. Fu. Cuffless blood pressure estimation based on photoplethysmography signal and its second derivative. *International Journal of Computer Theory and Engineering*, 9:202–206, 01 2017.
- [22] J. Masci et al. Stacked convolutional auto-encoders for hierarchical feature extraction. In *Artificial Neural Networks and Machine Learning – ICANN 2011*, pages 52–59, Berlin, Heidelberg, 2011. Springer Berlin Heidelberg.
- [23] F. Miao et al. A novel continuous blood pressure estimation approach based on data mining techniques. *IEEE Journal of Biomedical and Health Informatics*, PP:1–1, 04 2017.
- [24] J. L. Moraes et al. Advances in photoplethysmography signal analysis for biomedical applications. *Sensors*, 18(6), 2018.

- [25] S. S. Mousavi et al. Blood pressure estimation from appropriate and inappropriate ppg signals using a whole-based method. *Biomedical Signal Processing and Control*, 47:196–206, 2019.
- [26] V. Nair and G. E. Hinton. Rectified linear units improve restricted boltzmann machines. In *Proceedings of the 27th International Conference on International Conference on Machine Learning*, ICML’10, pages 807–814, USA, 2010. Omnipress.
- [27] E. O’Brien, B. Waeber, G. Parati, J. Staessen, and M. G. Myers. Blood pressure measuring devices: recommendations of the european society of hypertension. *BMJ*, 322(7285):531–536, 2001.
- [28] W. H. Organization et al. Global status report on noncommunicable diseases 2014. Technical report, World Health Organization, 2014.
- [29] S. Shimazaki, S. Bhuiyan, H. Kawanaka, and K. Oguri. Features extraction for cuffless blood pressure estimation by autoencoder from photoplethysmography. In *2018 40th Annual International Conference of the IEEE Engineering in Medicine and Biology Society (EMBC)*, pages 2857–2860. IEEE, 2018.
- [30] N. Srivastava, G. Hinton, A. Krizhevsky, I. Sutskever, and R. Salakhutdinov. Dropout: A simple way to prevent neural networks from overfitting. *Journal of Machine Learning Research*, 15:1929–1958, 2014.
- [31] A. Tazarv, S. Labbaf, A. M. Rahmani, N. Dutt, and M. Levorato. Data collection and labeling of real-time iot-enabled bio-signals in everyday settings for mental health improvement. In *Proceedings of the Conference on Information Technology for Social Good*, pages 186–191, 2021.
- [32] A. Tazarv, S. Labbaf, S. M. Reich, N. Dutt, A. M. Rahmani, and M. Levorato. Personalized stress monitoring using wearable sensors in everyday settings. In *2021 43rd Annual International Conference of the IEEE Engineering in Medicine & Biology Society (EMBC)*, pages 7332–7335. IEEE, 2021.
- [33] X. Xing and M. Sun. Optical blood pressure estimation with photoplethysmography and fft-based neural networks. *Biomedical optics express*, 7(8):3007–3020, 2016.
- [34] Y. Zhang and Z. Feng. A svm method for continuous blood pressure estimation from a ppg signal. In *Proceedings of the 9th International Conference on Machine Learning and Computing*, ICMLC 2017, pages 128–132, New York, NY, USA, 2017. ACM.
- [35] Z. Zhang, Z. Pi, and B. Liu. Troika: A general framework for heart rate monitoring using wrist-type photoplethysmographic signals during intensive physical exercise. *IEEE Transactions on biomedical engineering*, 62(2):522–531, 2014.